[CANCER RESEARCH 64, 3022–3029, May 1, 2004]

Apoptotic Signaling Pathways Induced by Nitric Oxide in Human Lymphoblastoid Cells Expressing Wild-Type or Mutant p53

Chun-Qi Li,[1] Ana I. Robles,[2] Christin L. Hanigan,[2] Lorne J. Hofseth,[2] Laura J. Trudel,[1] Curtis C. Harris,[2] and Gerald N. Wogan[1,2]

[1]Biological Engineering Division and Department of Chemistry, Massachusetts Institute of Technology, Cambridge, Massachusetts; and [2]Laboratory of Human Carcinogenesis, National Cancer Institute, NIH, Bethesda, Maryland

ABSTRACT

Loss of p53 function by inactivating mutations results in abrogation of NO•-induced apoptosis in human lymphoblastoid cells. Here we report characterization of apoptotic signaling pathways activated by NO• in these cells by cDNA microarray expression and immunoblotting. A p53-mediated transcriptional response to NO• was observed in p53-wild-type TK6, but not in closely related p53-mutant WTK1, cells. Several previously characterized p53 target genes were up-regulated transcriptionally in TK6 cells, including phosphatase *PPM1D* (WIP1), oxidoreductase homolog *PIG3*, death receptor *TNFRSF6* (Fas/CD95), and BH3-only proteins *BBC3* (PUMA) and *PMAIP1* (NOXA). NO• also modulated levels of several gene products in the mitochondria-dependent and death-receptor-mediated apoptotic pathways. Inhibitors of apoptosis proteins X-chromosome-linked inhibitor of apoptosis, cellular inhibitor of apoptosis protein-1, and survivin were significantly down-regulated in TK6 cells, but not in WTK1 cells. Smac release from mitochondria was induced in both cell types, but release of apoptosis-inducing factor and endonuclease G was detected only in TK6 cells. Fas/CD95 was increased, and levels of the antiapoptotic proteins Bcl-2 and Bcl-x/L were reduced in TK6 cells. Activation of procaspases 3, 8, 9, and 10, as well as Bid and poly(ADP-ribose) polymerase cleavage, were observed only in TK6 cells. NO• treatment did not alter levels of death receptors 4 and 5, Fas-associated death domain or proapoptotic Bax and Bak proteins in either cell line. Collectively, these data show that NO• exposure activated a complex network of responses leading to p53-dependent apoptosis via both mitochondrial and Fas receptor pathways, which were abrogated in the presence of mutant p53.

INTRODUCTION

NO• has been shown to initiate apoptotic cell death in many *in vitro* and *in vivo* experimental models (1, 2); however, the pathways involved are still not completely understood. Two major signaling pathways leading to apoptosis have been identified. One is mitochondria-dependent, resulting from release of mitochondrial proapoptotic proteins and leading to caspase-dependent and/or -independent apoptosis. The other is death receptor /caspase-8-dependent, involving the interaction of death receptors with receptor-associated death proteases and subsequent activation of downstream effector caspases (3, 4).

Wild-type p53 is a critical cellular gatekeeper for growth and division that mediates DNA damage-induced cell-cycle arrest and apoptosis (5) through, at least in part, the transcriptional activation of $p21^{WAF1}$, an inhibitor of cyclin-dependent kinases (6). Biochemical mechanisms underlying apoptotic responses activated by p53 remain incompletely characterized, although its transcriptional activity is clearly involved, as evidenced by the fact that most *TP53* mutations in human cancer are missense and map to the DNA binding domain of the protein (7). Among the many genes transcriptionally up-regulated in response to p53 activation, early studies showed the involvement of p53-inducible genes (*PIG*; Ref. 8), as well as Bax (9), Fas/CD95 (4), and death receptor 5 (DR5; Ref. 10) in apoptosis, whereas others indicated that neither Bax nor DR5 were absolutely required (11, 12) and argued that Fas/CD95 may be a downstream target of p53 (13, 14). Recent evidence suggests that death receptor 4 (DR4) may also be regulated by p53, and its expression induced by DNA damage (15). Lately, global analysis of gene expression after p53 activation has yielded numerous novel p53 transcriptional target genes, including some with clear proapoptotic properties, such as the BH3-only proteins *BBC3* (PUMA; Refs. 16, 17) and *PMAIP1* (NOXA; Ref. 18), the apoptotic protease-activating factor *APAF-1* (19, 20), and the serine protease *PRSS25* (HTRA2; Ref. 21). Still, neither the single-gene approach nor gene expression profiling alone has been shown to accurately reflect the complex network of responses that characterizes an apoptotic program.

Mitochondria play a central role in apoptotic events through release of the proapoptotic factors cytochrome *c*, Smac, apoptosis-inducing factor (AIF), and endonuclease G (3). The Bcl-2 family of proteins, comprising both antiapoptotic (Bcl-2 and Bcl-x/L) and proapoptotic (Bax, Bak, Bid, NOXA, and PUMA) members, integrates diverse cell death signals and regulates the integrity of mitochondrial membrane (3, 22). Activated p53 can directly or indirectly modulate the expression of these and other proteins that control mitochondrial membrane permeability and, therefore, the release of mitochondrial proteins during apoptosis (23). We previously found that NO• treatment resulted in mitochondrial membrane depolarization and cytochrome *c* release in a pair of closely related human lymphoblastoid cells harboring either wild-type (TK6 cells) or mutant p53 (WTK1 cells), but the apoptotic response was substantially different in the two cell types (24). In this study, we explore the involvement of the Bcl-2 family of proteins in NO•-induced cell death as well as release of the mitochondrial proapoptotic factors Smac, AIF, and endonuclease G. Smac promotes caspase activation by binding to inhibitors of apoptosis proteins (IAPs) and suppressing their antiapoptotic activity (25). AIF and endonuclease G translocate from mitochondria to nuclei during apoptosis, where they induce caspase-independent chromatin condensation and large-scale (50 kb) DNA cleavage (26–28).

The IAP family proteins X-chromosome-linked inhibitor of apoptosis (XIAP) and cellular inhibitor of apoptosis protein-1 (cIAP-1) are potent suppressors of apoptosis that act by directly inhibiting distinct caspases (29). Their caspase-inhibiting activity is negatively regulated by Smac (25). IAP family proteins also possess ubiquitin protein ligase (E3) activity and mediate their own ubiquitination and degradation in apoptosis induced by dexamethasone or etoposide in mouse thymocytes (30). Our previous study suggested that XIAP protein is down-regulated by p53 in NO•-induced apoptosis in human lymphoblasts (24). Additionally, two recent reports indicated that the IAP family member survivin is transcriptionally repressed by wild-type p53 and participates in p53-dependent apoptosis (31, 32).

Received 6/25/03; revised 1/14/04; accepted 3/2/04.

Grant support: Supported in part by Grant 5 P01 CA26731 from the National Cancer Institute.

The costs of publication of this article were defrayed in part by the payment of page charges. This article must therefore be hereby marked *advertisement* in accordance with 18 U.S.C. Section 1734 solely to indicate this fact.

Note: C-Q. Li and A. Robles contributed equally to this work. Supplementary data for this article can be found at Cancer Research Online (http://cancerres.aacrjournals.org).

Requests for reprints: Gerald Wogan, Massachusetts Institute of Technology, Biological Engineering Division and Department of Chemistry, Room 26-009, 77 Massachusetts Avenue, Cambridge, MA 02139-4307. Phone: (617) 253-3188; Fax: (617) 258-9733; E-mail: wogan@mit.edu.

We previously showed that apoptosis induced by NO• was delayed and greatly reduced in magnitude in WTK1 cells compared with TK6 cells (24). Separately, we also found that peroxynitrite generated by SIN-1 decomposition induced time-dependent apoptosis in TK6 cells but not in WTK1 cells (33). Other investigators have reported that p53 was involved in, but not required for, ionizing radiation-induced caspase-3 activation and apoptosis in the same cell lines (34). We conducted the present study to characterize more completely the signaling pathways affected by NO• exposure in TK6 and WTK1. We found that induction of apoptosis by NO• treatment in TK6 cells correlated with activation of both mitochondria-dependent and Fas/CD95 (but not DR4 and -5)/caspase-8-dependent pathways. The involvement of both pathways was evidenced by transcriptional upregulation of p53 target genes. Moreover, levels of IAP, AIF, Fas/CD95, Bid, Bcl-2, and Bcl-x/L proteins, but not of Bax, Bak, DR4, and DR5 proteins, were affected by NO• in p53-wild-type TK6 cells but remained unchanged in p53-mutant WTK1 cells. Apoptosis was much delayed and diminished in WTK1 cells, although they still showed an early transcriptional response to NO• and release of certain apoptogenic factors. Therefore, a complex network of p53-dependent and -independent pathways are modulated by NO• exposure and contribute to the apoptotic response in lymphoblastoid cells.

MATERIALS AND METHODS

Cell Culture. TK6 cells were kindly provided by Dr. W. G. Thilly (Massachusetts Institute of Technology, Cambridge, MA) and WTK1 cells by Dr. H. L. Liber (Colorado State University, Fort Collins, CO). They are EBV-immortalized human lymphoblastoid cell lines derived from the same donor. WTK1 cells contain a C-to-T transition in exon 7 of *TP53*, which results in a change of Met to Ile at codon 237 of p53, leading to accumulation of a nonfunctional protein. All cell culture reagents were purchased from BioWhittaker (Walkersville, MD). Cells were maintained in exponentially growing suspension culture at 37°C in a humidified, 5% CO_2 atmosphere in RPMI 1640 supplemented with 10% heat-inactivated calf serum, 100 units/ml penicillin, 100 μg/ml streptomycin, and 2 mM L-glutamine. Stock cells were subcultured and maintained at a density not greater than 1.5×10^6 cells/ml in 150-mm dishes throughout experiments.

NO• Treatment. NO• treatment was as described previously (24). Briefly, cells at a density of 4×10^5 cells/ml in 100 ml of custom RPMI 1640 without calcium nitrate (Life Technologies) and calf serum were exposed to pure NO• gas (Matheson, Gloucester, MA) by diffusion through Silastic tubing (0.025-inch inner diameter; 0.047-inch outer diameter; Dow Corning, Midland, MI) delivery system. NO• diffuses through this permeable membrane at a constant rate, and was delivered through 30-cm-long tubing into the medium of well-stirred cell suspensions for 2 h. Cells similarly exposed to argon gas served as negative controls. Total dose (and rate) of NO• delivered under these conditions was 390 μmol (533 nM/s), calculated from the nitrite plus nitrate content of the medium as determined by automated analysis using the Griess reagent [*N*-(1-napthy)-ethylenediamine and sulfanilic acid] (35). At the end of treatment, cells were collected by centrifugation, washed once, resuspended in fresh culture medium containing 10% heat-inactivated calf serum, and incubated at 37°C. At the indicated times, cells were washed in cold PBS, harvested, and stored at −80°C for RNA or protein extraction.

cDNA Microarray Hybridization. Cells were lysed with TRIzol reagent (Invitrogen, Carlsbad, CA), and total RNA was extracted according to the manufacturer's instructions at 0, 6, 12, and 24 h after NO• treatment. Fluorescently labeled cDNA probes were generated with 40 μg of total RNA by a single round of reverse transcription in the presence of aminoallyl-dUTP (Sigma, St. Louis, MO), followed by a coupling reaction to Cy3 or Cy5 monofunctional *N*-hydroxysuccinimide ester (Amersham Pharmacia, Piscataway, NJ). Complex probes (usually containing untreated Cy3-labeled cDNA and NO•-treated Cy5-labeled cDNA) were denatured, hybridized to glass slides featuring 9180 cDNA clones based on the Hs Unigene build #131 platform (7102 "named" genes, 1179 expressed sequence tag clones, and 122 Incyte clones), and printed by the National Cancer Institute Microarray Facility, Advanced Technology Center, Gaithersburg, MD. After overnight incubation at 42°C, the slides were washed successively in 1× SSC–0.1% SDS, 1× SSC, and 0.2× SSC for 2 min each, then rinsed in 0.5× SSC and spin-dried. The two fluorescent intensities were measured simultaneously with a GenePix 4000A scanner, and the acquired image was processed with GenePix Pro 3.0 software (Axon Instruments, Union City, CA). The basic raw data and derived ratio measurements were then uploaded to the National Cancer Institute MicroArray Database system for normalization and data extraction in formats compatible with microarray analysis tools.

cDNA Microarray Analysis and Statistics. After determination of the overall quality of the arrays by visual inspection and signal-to-background ratios, spot size and intensity filters were applied to all measurements in each array. Hybridization quality replicates consisting of the same RNA samples applied to two independent arrays as well as exposure reproducibility replicates consisting of separate samples simultaneously exposed on parallel delivery systems or completely independent exposures (done on different days from freshly grown cells) were used to minimize random fluctuations in gene expression. The overall array similarity was assessed by Pearson correlation coefficient. Hybridization quality replicates showed Pearson correlation coefficients >0.8, whereas the correlation among completely independent exposures of the same cell line showed Pearson correlation coefficients of 0.6–0.7.

Unsupervised and supervised analysis algorithms were used to identify genes and signaling pathways affected by NO• exposure. For unsupervised analysis of expression trends across time points in both cell lines, genes were selected based on an arbitrary threshold of up- or down-regulation of their normalized Cy5:Cy3 ratios and were subjected to hierarchical clustering analysis using CLUSTER and TREEVIEW software (36). We used the BRB Array Tools software developed by the Biometric Research Branch of the National Cancer Institute for the supervised analysis. This is an integrated package for the visualization and statistical analysis of cDNA microarray gene expression data. We used the Class Comparison Tool based on univariate *F* tests to identify genes differentially expressed between TK6 and WTK1 at 24 h after NO• exposure. The permutation distribution of the *F* statistic, based on 1000 random permutations, was also used to confirm statistical significance.

Quantitative Real-Time Reverse Transcription-PCR. For validation of cDNA microarray results, cDNA was prepared by reverse transcription with oligo(dT) primer (Promega, Madison, WI) using 4 μg of total RNA extracted at 0, 6, 12, and 24 h after NO• treatment. Each PCR was carried out in triplicate in a 20-μl volume using Sybr Green Mastermix (Applied Biosystems, Foster City, CA) on the ABI Prism 7700 Sequence Detection System with standard parameters. The sequences of the primers used were as follows: *BBC3* forward, 5′-GACTGTGAATCCTGTGCTCTGC-3′; *BBC3* reverse, 5′-CGTCGCTCTCTCTAAACCTATGC-3′; *PPM1D* forward, 5′-TCGCTTGTCACCTTGCCAT-3′; *PPM1D* reverse, 5′-TGTGCTAGGAAGACCCGTCAT-5′; *PMAIP1* forward, 5′-GCTCCAGCAGAGCTGGAAGT-3′; *PMAIP1* reverse, 5′-GAAGTTTCTGCCGGAAGTTCA-3′; *PIG3* forward, 5′-CGCTGAAATTCACCAAAGGTG-3′; and *PIG3* reverse, 5′-AACCCATCGACCATCAAGAGC-3′. Dissociation curves and no-cDNA controls were generated for each primer pair to detect nonspecific amplification. A standard curve was generated for each primer pair as well as for glyceraldehyde-3-phosphate dehydrogenase (*GAPDH*; using in this case a predeveloped TaqMan assay), to which gene expression levels were normalized by a comparative threshold cycle method. Finally, a ratio was calculated comparing normalized gene expression values in treated *versus* untreated control for each cell line.

Antibodies. Antibodies used for immunoblotting were purchased as follows: monoclonal anti-caspase 8, rabbit antihuman p53-phosphoserine 15, and monoclonal antibodies against XIAP, FADD, Bid, Bax, Bcl-x/L, Smac, caspase 10, caspase 3, and poly(ADP-ribose) polymerase (PARP) were from Cell Signaling Technology (Beverly, MA); affinity-purified rabbit antihuman/mouse cIAP-1 and rabbit antihuman survivin were from R&D Systems (Minneapolis, MN); rabbit anti-AIF and anti-endonuclease G were from ProSci Incorporated (Poway, CA); mouse anti-heat shock protein 60 monoclonal and rabbit anti-Fas, -DR4, and -DR5 were from StressGen Biotechnologies Corp (Victoria, BC, Canada); monoclonal antihuman p53 antibody (Ab-6), anti-Bcl-2 (Ab-3), anti-MDM2 (Ab-2), and antiactin (Ab-1) were from Oncogene (Cambridge, MA); purified mouse antihuman caspase 9 monoclonal was from PharMingen (San Diego, CA); affinity-purified rabbit antihuman Bak was from R&D Systems and Santa Cruz Biotechnology (Santa Cruz, CA); and goat

and rabbit antimouse IgG conjugated to horseradish peroxidase were from Bio-Rad (Hercules, CA).

Whole-Cell Extract and Cytosolic and Mitochondrial Fraction Preparation. Cells were lysed in 100 μl of cold CHAPS Cell Extract Buffer [50 mM Pipes-KOH (pH 6.5), 2 mM EDTA, 0.1% CHAPS, 20 mg/ml leupeptin, 10 mg/ml pepstatin A, and 10 mg/ml aprotinin, supplemented with 5 mM DTT and 1 mM phenylmethylsulfonyl fluoride; Cell Signaling Technology] for 30 min on ice, and then were subjected to three freeze–thaw cycles in liquid nitrogen and a 37°C water bath. The whole-cell lysate was centrifuged at 14,000 rpm for 10 min at 4°C, and the protein concentration in the resulting supernatant was measured with Bio-Rad protein assay before immunoblotting analysis. Cytosolic fractions were prepared as described previously (24) and stored at −80°C for Smac analysis. Mitochondrial pellets separated from the cytosolic fraction were lysed with 100 μl of buffer B [50 mM HEPES (pH 7.4), 1% (v/v) NP40, 10% (v/v) glycerol, 1 mM EDTA, and 2 mM DTT] supplemented with a fresh cocktail of protease inhibitors (Roche Diagnostics GmbH, Mannheim, Germany). Samples were vortex-mixed from time to time during the 20-min incubation period on ice. Cellular debris was removed by centrifugation at 22,000 × *g* for 15 min at 4°C, and the resulting supernatants containing mitochondrial proteins were saved for AIF and endonuclease G analysis.

Western Blot Analysis. For Western blot analysis, 50 μg of proteins from the whole-cell lysate or the cytosolic or mitochondrial fractions were denatured, resolved on 15% SDS-PAGE gels, and electrotransferred at 180 mA for 1 h onto a polyvinylidene difluoride membrane (Bio-Rad). Blots were probed with appropriate primary antibodies overnight at 4°C, followed by a secondary goat antirabbit or mouse IgG conjugated to horseradish peroxidase and determination of supersignal ultrachemiluminescence (Pierce, Rockford, IL) by exposure to Hyperfilm ECL (Amersham Pharmacia, Piscataway, NJ; Ref. 24). All primary antibodies were diluted to a concentration of 1:1000 except for anti-Fas (1:2000), and -DR4 (1:1500); anti-cIAP-1, -survivin, and -AIF were used at a concentration of 1 μg/ml. To control for protein loading, membranes were stripped and reprobed with antiactin (1:10,000 dilution) or anti-heat shock protein 60 antibody (1 μg/ml). Densitometric values for appropriate bands on Western blots were quantified by Scion Image β 4.02 software.[3]

Statistical Analysis. Data values for quantitative real-time reverse transcription-PCR and Western blotting are expressed as means ± SD. Statistical analysis was performed with a two-tailed Student's *t* test, and $P < 0.05$ was considered statistically significant.

RESULTS

Global Expression Profiling after Exposure to NO•. We used gene expression profiling[4] to determine which genes and signaling pathways were affected by exposure of lymphoblastoid cells to NO•. From our previous data indicating a strong apoptotic response in p53-wild-type TK6 cells after exposure to NO• and its delay and decrease in related p53-mutant WTK1 cells (24), we hypothesized that NO• would activate a p53-mediated transcriptional response. We therefore selected the time frame for the analysis based on a preliminary study of the kinetics of p53 protein accumulation in response to NO• (Supplementary Data Fig. 1). Gene expression was analyzed in TK6 and WTK1 cells by cDNA microarray hybridization using total RNA extracted at 6, 12, and 24 h after exposure to NO• or 24 h after exposure to argon to control for nontreatment-specific gene fluctuations. In each case, complex probes were generated containing Cy5-labeled cDNA derived from NO•- or argon-treated cells and Cy3-labeled cDNA from the corresponding untreated cells.

For the analysis of temporal patterns of gene expression, 136 genes were selected based on an arbitrary threshold of 2-fold up- or down-regulation of normalized Cy5:Cy3 ratios in at least one of the time points in either TK6 or WTK1 cells, using averaged gene expression values for duplicate arrays at each time point, and a criterion of genes present (after spot size and intensity filters) in at least 80% of the averaged arrays. Fig. 1 shows a graphic view in pseudo-color of gene expression clusters generated through a hierarchical algorithm that groups genes according to the similarities in their patterns of expression. In this type of analysis, genes belonging to a similar functional category tend to cluster together. Three main clusters that are specific for NO• treatment (not present in cells treated with argon) and correlate with length of incubation after exposure can be clearly distinguished in this display. The first group of genes (cluster I) represents an early transcriptional response that may not require protein synthesis and is independent of wild-type p53 (*i.e.,* genes induced in both TK6 and WTK1 cells). Their expression peaks at 6 h after exposure and declines at later time points. The genes in the second group (cluster II) are induced with opposite kinetics (their expression rises steadily and peaks at 24 h after exposure) and are preferentially up-regulated in p53-wild-type TK6 cells. Lastly, there is a small cluster of genes (cluster III) with strong activation only in TK6 cells at 24 h after exposure. Many of the genes in cluster I code for transcription factors and include several C2H2-type and Kruppel-like zinc finger proteins; *BATF*, a basic leucine zipper protein that belongs to the AP-1/ATF superfamily of transcription factors; and *HIF1A*, the basic helix-loop-helix protein that activates transcription of hypoxia-inducible genes. Cluster II features several known p53 target genes, such as *CDKN1A* ($p21^{WAF1}$), *MDM2*, *PPM1D* (WIP1), *ENC1* (PIG10), *GADD45*, *TNFRSF6* (Fas/CD95), and *PMAIP1* (NOXA). No single category characterizes the genes in cluster III, which include the DNA replication and repair factor *PCNA* and the Bcl-2-interacting protein *BNIP2*. Taken together, these data indicate that there are distinct signaling pathways activated by NO• exposure that differ in terms of their dependence on wild-type p53.

To assess statistical significance to the observed wild-type p53-dependent up-regulation of genes in TK6 cells, we applied a supervised class comparison analysis with univariate *F* tests and a global permutation test. A comparison of five replicate treatments of TK6 cells and three replicate treatments of WTK1 cells 24 h after exposures yielded a total of 75 significant genes ($P < 0.001$). Permutation analysis showed that there was a low overall probability ($P < 0.02$) that these differences could have occurred by chance. Visual inspection of the list revealed that 9 of those 75 genes (12%) are known p53 transcriptional target genes, whereas a total of 29 genes (0.40% of 7102) were identified within the entire list of named genes in the array as previously characterized p53 transcriptional target genes. Table 1 shows the identities, the average ratio values of gene expression at 24 h after exposure to NO•, and the parametric *P*s for genes identified as known p53 transcriptional targets (see Supplementary Data Table 1 for complete listing). Our analysis indicates that it is possible to recognize a wild-type p53 transcription signature in TK6 cells after exposure to NO•.

Validation of Microarray Results for Selected p53 Target Genes. Quantitative real-time reverse transcription-PCR confirmed that selected p53-inducible genes from Table 1 were up-regulated preferentially in NO•-treated TK6 cells (Fig. 2). These genes were chosen based on their proapoptotic properties (*NOXA* and *PUMA*) and their potential specificity for activation after treatment with NO• (*WIP1* and *PIG3*). There was up to a 2.5-fold induction of *NOXA* in both TK6 and WTK1 cells after 6 h of NO• treatment; however, *NOXA* continued to increase in TK6 cells up to 5-fold at 12 h, whereas it decreased in WTK1 cells. *WIP1*, *PUMA* and *PIG3* were up-regulated essentially only in TK6 cells.

Taken together, the mRNA expression studies indicate that both mitochondrial and receptor-mediated pathways of apoptosis were activated through p53-mediated transcription in TK6 cells. To confirm

[3] Downloaded from http://www.scioncorp.com.

[4] The original data will be available on the National Center for Biotechnology Information Gene Expression Omnibus public database (http://www.ncbi.nlm.nih.gov/geo) as GSE1064.

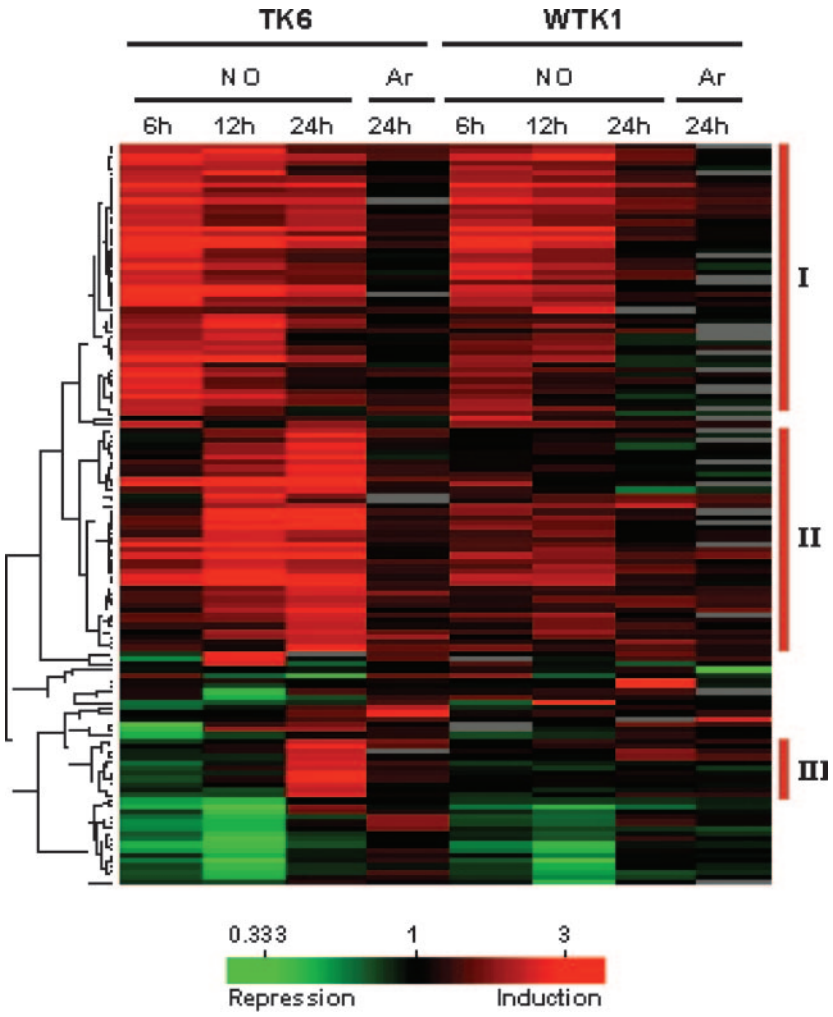

Fig. 1. Hierarchical clustering of gene expression profiles in TK6 and WTK1 cells after NO• or argon (*Ar*) treatment. A total of 136 genes selected based on an arbitrary threshold of 2-fold up- or down-regulation in at least one time point in either cell line were clustered into groups representing temporal expression patterns. The degree of expression compared with untreated control is color-coded, as displayed at the *bottom* of the figure.

and extend these findings, we then analyzed the expression of selected proteins belonging to both apoptotic pathways.

Protein Expression Changes Associated with NO• Exposure. The stabilization and activation of p53 protein as a transcription factor is characterized by the appearance of post-translationally modified forms of the protein, which are detectable with epitope-specific antibodies. The most characteristic post-translational modification after NO• exposure is phosphorylation at Ser-15 (37) which interferes with p53 binding to MDM2 and its subsequent degradation. *MDM2* is also a p53 transcriptional target, creating a negative feedback loop that ensures down-regulation of the p53 DNA damage response (38, Table 1). Wild-type p53 protein levels increased progressively in TK6 cells through 24 h after NO• treatment, reaching a maximum elevation of 200% compared with argon-treated cells; the high basal level of mutant p53 protein in WTK1 cells showed no further increase after the same treatment (Table 2). Accumulation of p53 was accompanied by phosphoserine 15 modification (Supplementary Data Fig. 1). Conversely, MDM2 protein declined gradually, with maximum losses of 58% in TK6 cells and 21% in WTK1 cells 24 h after NO• treatment (Table 2). These findings, together with greater decreases in procaspase 3 and full-length PARP levels (Table 2), are consistent with our previous observations of faster and more pronounced apoptosis in TK6 cells than in WTK1 cells (24) and with the finding that NO• treatment can induce elevated expression of wild-type p53 through an initial down-regulation of MDM2 that is independent of p53 (39).

Table 1 *Average ratio values of gene expression in TK6 and WTK1 cells for selected known p53-transcriptional target genes 24 h after exposure to NO•*

		Ratio of gene expression[a]		
UNIGENE	Gene name	TK6	WTK1	P^b
Hs.96	*PMAIP1* (NOXA)	2.5 ± 0.8	1.1 ± 0.1	1×10^{-6}
Hs.100980	*PPM1D* (WIP1)	3.0 ± 0.6	1.2 ± 0.2	1×10^{-6}
Hs.179665	*CDKN1A* ($p21^{WAF1}$)	4.4 ± 1.4	1.3 ± 0.2	3×10^{-6}
Hs.94262	*RRM2B* (p53R2)	1.8 ± 0.2	0.9 ± 0.1	7×10^{-6}
Hs.77602	*DDB2*	1.8 ± 0.4	1.0 ± 0.1	0.0001
Hs.82359	*TNFRSF6* (FAS/CD95)	2.5 ± 0.8	1.2 ± 0.1	0.0001
Hs.87246	*BBC3* (PUMA)	1.7 ± 0.1	1.1 ± 0.2	0.0002
Hs.104925	*ENC1* (PIG10)	2.7 ± 0.6	1.6 ± 0.4	0.0004
Hs.69745	*FXDR*	1.3 ± 0.3	0.8 ± 0.1	0.0007
Hs.76686	*GPX1*	1.4 ± 0.2	1.0 ± 0.1	0.003
Hs.51233	*TNFRSF10B* (DR5)	1.5 ± 0.4	1.0 ± 0.1	0.004
Hs.170027	*MDM2*	2.8 ± 1.5	1.0 ± 0.1	0.005
Hs.80409	*GADD45A*	2.0 ± 0.7	1.3 ± 0.1	0.007
Hs.50649	*PIG3*	2.4 ± 0.9	1.2 ± 0.1	0.007

[a] Compared with argon-treated control. Values are mean ± SD from five (TK6) or three (WTK1) independent experiments.
[b] Parametric *P*s obtained through class comparison analysis are shown.

The responses of gene products in the apoptotic signaling pathways of TK6 and WTK1 cells after exposure to NO• are summarized in Tables 2 and 3 and in Figs. 3–5. The IAP family members XIAP, cIAP-1, and survivin were prominently expressed in argon-treated cells harboring either wild-type (TK6 cells) or mutant (WTK1 cells) p53. The XIAP protein level was substantially down-regulated after NO• treatment in TK6 cells (Table 2). Levels of cIAP-1 and survivin proteins were also reduced by 17–69% and 55–67%, respectively (Fig. 3). In contrast, in WTK1 cells, levels of these gene products

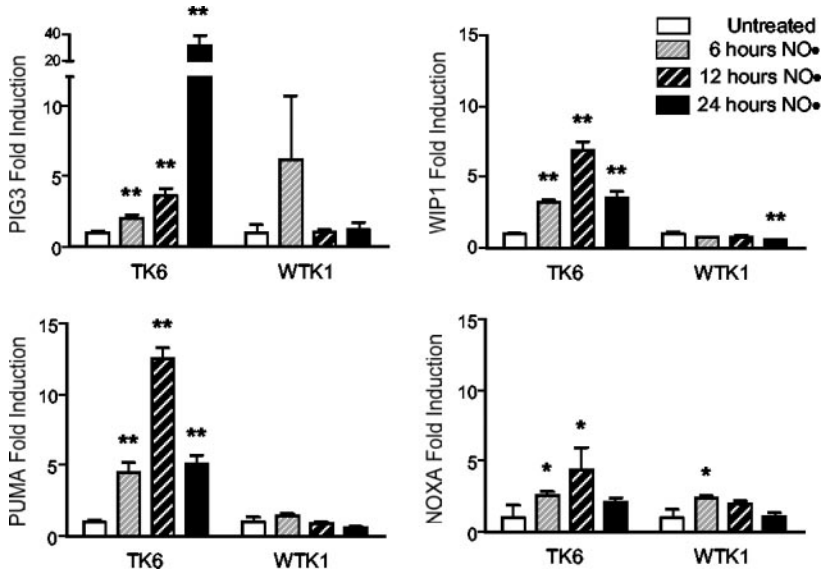

Fig. 2. Validation of microarray analysis by quantitative real-time reverse transcription-PCR. Fold induction *versus* untreated control of normalized gene expression of selected p53-target genes in TK6 and WTK1 cells after NO• treatment. Mean ± SD (*bars*) are shown. *, $P < 0.05$; **, $P < 0.01$ compared with untreated control cells.

Table 2 *Gene products significantly altered in TK6 cells, but not WTK1 cells by NO• treatment*

	Percentage of levels in argon-treated control cells[a]			
	TK6 cells		WTK1 cells	
Protein	4 h[b]	24 h[b,c]	4 h[b]	24 h[b]
p53	124 ± 8	200 ± 17	96 ± 1	99 ± 1
MDM2	83 ± 25	42 ± 3	93 ± 11	79 ± 16
Bcl-2	82 ± 16	70 ± 4	99 ± 1	93 ± 5
Bcl-x/L	84 ± 13	37 ± 19	91 ± 16	92 ± 13
Procaspase 9	79 ± 21	16 ± 11	96 ± 1	99 ± 1
Procaspase 3	90 ± 6	48 ± 19	92 ± 12	87 ± 1
PARP[d]	89 ± 16	45 ± 11	103 ± 8	94 ± 7
XIAP	75 ± 35	30 ± 7	98 ± 2	97 ± 1
Procaspase 8	88 ± 21	44 ± 12	92 ± 8	66 ± 21
Procaspase 10	95 ± 1	25 ± 17	90 ± 6	78 ± 11

[a] Values are means ± SD of two or three independent experiments.
[b] Time after the end of NO• treatment.
[c] All values are significantly different ($P < 0.05$ or $P < 0.01$) from values for argon-treated controls.
[d] PARP, poly(ADP-ribose) polymerase; XIAP, X-chromosome-linked inhibitor of apoptosis.

Table 3 *Gene products unaffected by exposure to NO• in either TK6 or WTK1 cells*[a]

	Percentage of levels in argon-treated control cells[b]			
	TK6 cells		WTK1 cells	
Protein	4/6 h[c]	24 h[c]	4/6 h[c]	24 h[c]
Bax	102 ± 1	99 ± 4	100 ± 3	99 ± 1
Bak	96 ± 2	99 ± 4	97 ± 1	101 ± 0
DR4[d]	101 ± 8	100 ± 7	100 ± 6	104 ± 2
DR5	97 ± 6	98 ± 6	102 ± 2	105 ± 4
FADD	98 ± 1	90 ± 14	100 ± 6	99 ± 11

[a] $P > 0.05$ for all, compared with argon-treated controls.
[b] Values are means ± SD from two independent experiments.
[c] Time after the end of NO• treatment.
[d] DR4 and DR5, death receptors 4 and 5, respectively.

were unaffected by treatment (Table 2; Fig. 3). Smac release from mitochondria into the cytosol was induced in both cell types, although it was more pronounced in WTK1 cells (Fig. 4). Substantial amounts of AIF and endonuclease G proteins were detected in the mitochondria of argon-treated TK6 and WTK1 cells, but after NO• treatment their levels decreased progressively in TK6 cells, with losses of 7–27% (AIF) and 6–74% (endonuclease G) occurring over periods of 6–24 h. In contrast, levels of these gene products remained essentially unchanged in mitochondria of NO•-treated WTK1 cells (Fig. 4). Pro-caspase 9 protein levels were reduced by 21–84% in TK6 cells but did not change in WTK1 cells during the 24-h period after NO• treatment (Table 2).

Fas/CD95 protein was detectable in argon-treated control cells of both types, and after NO• treatment, levels increased 317% at 6 h, subsequently decreasing to 212% at 12 h and returning to levels seen in control cells at 24 h in TK6 cells (Fig. 5). No significant alteration was noted in WTK1 cells during the same period. In contrast, levels of the DR4 and DR5 proteins as well as their adaptor protein FADD did not change in either cell type during the 24 h after treatment (Table 3). The receptor-associated proteases procaspase 8 and procaspase 10 were cleaved, and thus activated, after NO• exposure of both cell types, although the changes in WTK-1 cells were not

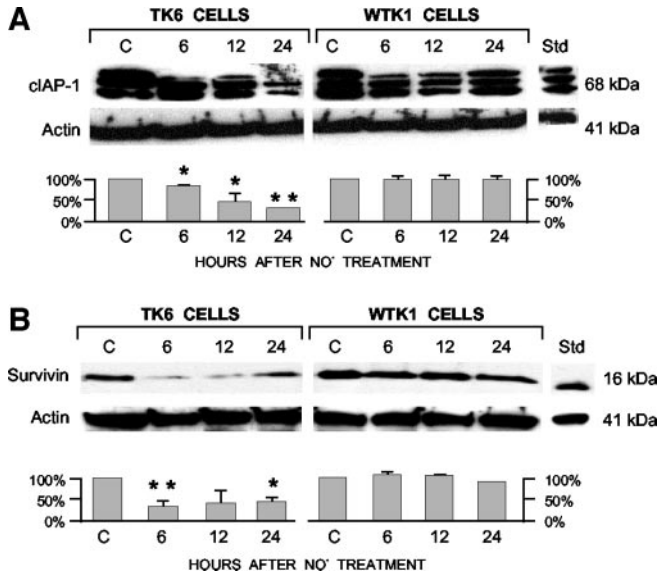

Fig. 3. Immunoblot analysis of levels of cIAP-1 (*A*) and survivin (*B*) proteins in lysates of TK6 and WTK1 cells after NO• treatment. Two to three bands of similar molecular weight may represent isoforms of cellular inhibitor of apoptosis protein-1 (*cIAP-1*) protein. Lysates of argon-treated lymphoblastoid cells and Jurkat cells treated with 4 μM staurosporine served as negative and positive controls, respectively. *Bar graphs* show changes from negative controls. Values are mean quantitative densitometric values and 95% confidence intervals (*bars*) from two independent experiments. *, $P < 0.05$; **, $P < 0.01$ compared with argon-treated controls (*columns* and *lanes* labeled as *C*). *Std*, standard.

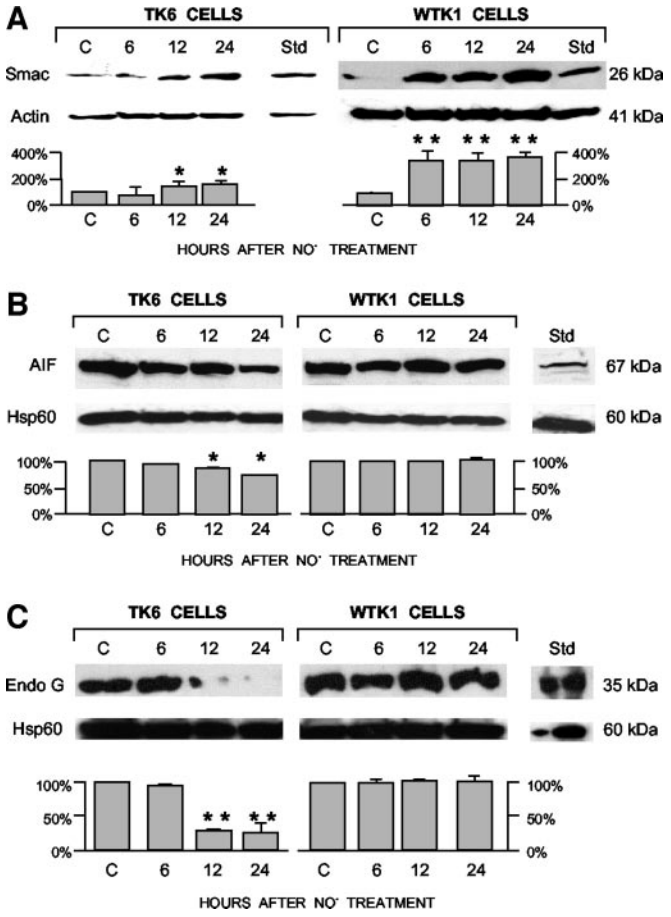

Fig. 4. Release of mitochondrial protein Smac into cytosol in TK6 and WTK1 cells (*A*) but loss of mitochondrial apoptosis-inducing factor (*AIF*; *B*) and endonuclease G (*Endo G*; *C*) proteins was observed only in TK6 after NO• treatment. A431 human epidermoid carcinoma cells served as a positive control for AIF, and HepG2 human hepatocellular carcinoma cells for endonuclease G. Negative controls and densitometric analyses are as indicated in the legend for Fig. 3. *, $P < 0.05$; **, $P < 0.01$ compared with argon-treated controls (*columns* and *lanes* labeled as *C*). *Hsp60*, heat shock protein 60; *Std*, standard.

statistically significant ($P > 0.05$; Table 2). Full-length Bid protein levels decreased 5–22% from control levels in TK6 cells, whereas they remained essentially unchanged in WTK1 cells (Fig. 5).

NO• treatment resulted in an 18–30% reduction of Bcl-2 protein and a 16–63% reduction of Bcl-x/L protein over periods of 4–24 h in TK6 cells, but neither protein level was altered in WTK1 cells (Table 2). In contrast, levels of the proapoptotic Bax and Bak proteins remained unchanged in both cell lines after NO• treatment (Table 3).

DISCUSSION

Taken together, our mRNA and protein analyses of lymphoblastoid cells undergoing apoptosis indicate that both mitochondria- and receptor-mediated pathways of apoptosis are activated by exposure to NO• and modulated by p53. We attribute the differences in responses of TK6 and WTK-1 cells to NO• treatment to their differing p53 status, because these cell lines were derived from the same donor source and thus are closely related. However, because both cell lines have been in culture for many years, contributions by factors other than p53 status cannot be completely ruled out. Several features of the data support our interpretation. p53 protein was activated and accumulated in TK6 cells upon exposure to NO• with kinetics consistent with the induction of p53-mediated transcription observed through microarray and reverse transcription-PCR analyses, which was abrogated in p53-mutant WTK1 cells. Furthermore, the transcriptional profile was driven by wild-type p53 at the time of maximum accumulation of p53 protein. This included the up-regulation of previously characterized p53 transcriptional targets that will be subjects of future studies. The large frequency of p53 target genes within genes up-regulated in TK6 cells implies that the p53-mediated transcriptional response is a main component of the apoptotic response to NO• exposure.

In particular, the BH3-only proteins NOXA and PUMA are known to contribute directly to mitochondrial membrane depolarization, followed by release of cytochrome *c* and apoptosis (22). A strong induction of PUMA in TK6 cells is consistent with its essential role in mediating p53-induced apoptosis in colorectal cancer cells, in which genetic disruption of *BBC3* completely abrogates apoptosis induced by exogenous p53 or by DNA damage (40). NOXA was up-regulated at early time points in WTK1 cells as well as TK6 cells, which indicates a p53-independent mechanism and may explain the fact that these cells show mitochondrial release of cytochrome *c* and Smac after NO• exposure, although WTK-1 cells are less sensitive to apoptosis (24). The WIP1 phosphatase participates in a negative feedback loop that suppresses the activation of p53 and p38 mitogen-activated protein kinase after treatment with UV radiation (41). The induction of WIP1 in TK6 cells was more pronounced after exposure to NO• or ionizing radiation than to doxorubicin (20), suggesting that activation of some p53 targets, such as WIP1, may be unique to certain DNA-damage response stress pathways. The oxidoreductase homolog PIG3 is involved in the modulation of oxidative stress (8, 42), and its strong induction in TK6 cells may contribute to the increased oxidative stress that characterizes NO• metabolism (42, 43).

The present study offers further support for the proposal that *TNFRSF6* is a p53-regulated gene (4) by showing evidence from both mRNA and protein analyses that activated p53 in TK6 cells up-regulated Fas/CD95. In contrast, levels of the DR4 and DR5 proteins as well as their adaptor protein FADD were not affected by p53 status, conflicting with reports that DR4 and DR5 are DNA damage-inducible, p53-up-regulated genes (10, 15) and with the modest up-regulation of *TNFRSF10B* (DR5) observed in the microarray analysis. Others have demonstrated both p53-dependent and -independent regulation of *DR5* gene expression in response to genotoxic stress and tumor necrosis factor α (12). These discrepancies suggest that mod-

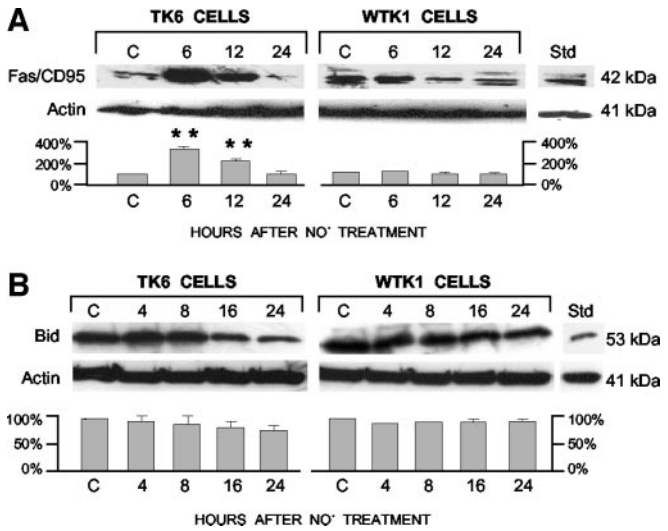

Fig. 5. Immunoblot analysis of Fas/CD95 (*A*) and Bid (*B*) proteins in lysates of TK6 and WTK1 cells after NO• treatment. Positive and negative controls (*lanes* and *columns* labeled as *C*) as well as densitometric analyses are as indicated in the legend for Fig. 3. **, $P < 0.01$ compared with argon-treated controls. Bid protein levels decreased from control levels in TK6 cells, but with marginal statistical significance ($P = 0.057$ at 24 h). *Std*, standard.

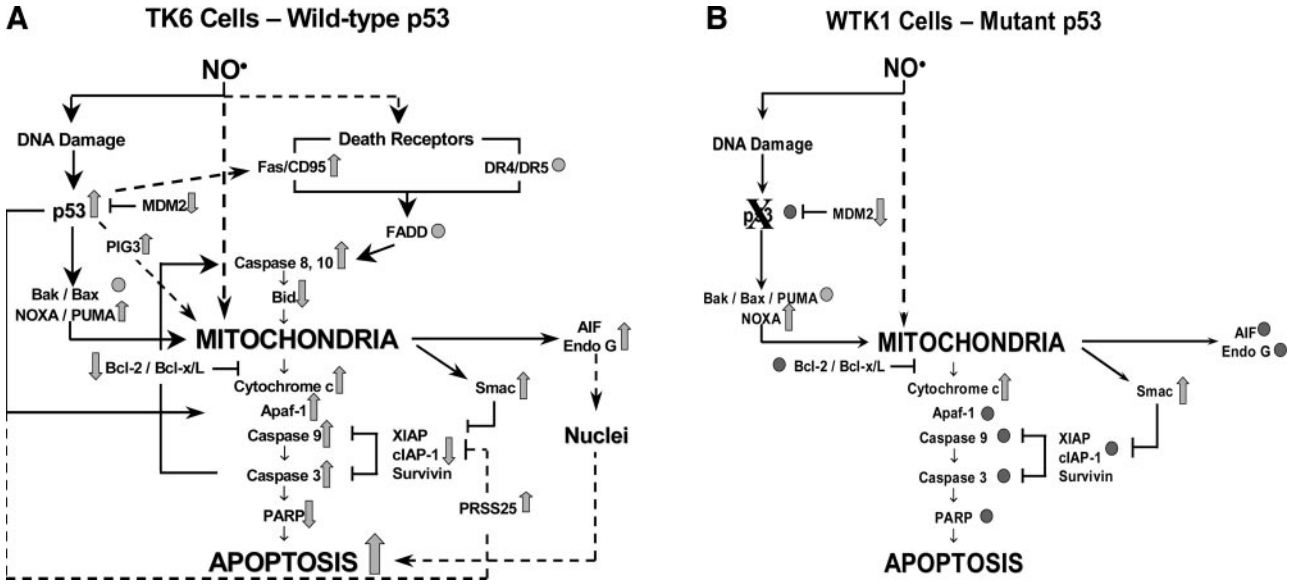

Fig. 6. Schematic summary of alterations in apoptosis signaling pathways induced by NO• treatment of TK6 and WTK1 cells. *Arrows* indicate substantial increases or decreases in protein level and extent of apoptosis. *Filled circles* indicate no change in these parameters. *Solid lines* indicate previously established interactions, and *dashed lines* indicate postulated interactions based on present experimental results. *DR4* and *DR5*, death receptors 4 and 5, respectively; *AIF*, apoptosis-inducing factor; *Endo G*, endonuclease G; *Apaf*, apoptotic protease-activating factor; *XIAP*, X-chromosome-linked inhibitor of apoptosis; *cIAP-1*, cellular inhibitor of apoptosis protein-1; *PARP*, poly(ADP-ribose) polymerase.

ulation of DR4 and DR5 by activated p53 may be inducer- and cell-type-specific or that they show delayed kinetics compared with Fas/CD95. Fas/CD95 activates caspases 8 and 10, which cleave Bid to truncated Bid, which in turn translocates onto mitochondria and leads to release of mitochondrial proapoptotic proteins and apoptosis (44).

Our data reveal that the IAP family proteins XIAP, cIAP-1, and survivin were down-regulated by functional p53 in TK6 cells, confirming and extending our earlier findings regarding the effects of NO• treatment on XIAP expression (24) and suggesting that these IAP family members are important intermediaries in the p53-dependent apoptotic response in these cells. NO• delivered from donor drugs has been shown to down-regulate levels of XIAP and cIAP-1 in lipopolysaccharide/IFN-γ-stimulated RAW 264.7 macrophages expressing wild-type p53 (45). The relevance of these findings is underscored by observations that both overexpression of IAP proteins and p53 mutations are associated with progressive development of many cancers (29, 32, 46) and that down-regulation of XIAP induces apoptosis in chemoresistant human ovarian cancer cells (47). We found no evidence for NO•-mediated transcriptional regulation of IAP genes in TK6 cells through either cDNA microarray or real-time PCR studies (data not shown). However, the serine protease *PRSS25* (HTRA2) was transcriptionally up-regulated in TK6 cells, albeit with a low statistical significance (data not shown). This was also the case for other p53 target genes, such as *GADD45* (Table 1) and *APAF-1* (data not shown). The HTRA2 protein interacts with and cleaves various IAP proteins, relieving caspase inhibition and activating apoptosis (21, 48). Thus, the modulation of IAP proteins by p53 may occur through different pathways in specific systems. Further research will be required to evaluate these and other possible mechanisms.

NO• treatment induced cytochrome *c* (24) and Smac release from mitochondria into cytosol in both TK6 and WTK-1 cells, but loss of the mitochondrial AIF and endonuclease G proteins was observed only in TK6 cells. These data indicate that complex mechanisms control release of mitochondrial proapoptotic factors but suggest that expression and/or release of AIF and endonuclease G proteins may be modulated by p53. p53 modulation may be mediated through regulation of Bcl-2, which has been shown to prevent mitochondrial–nuclear redistribution of AIF (26, 49). *APAF-1* has been identified as a p53 response gene (19, 20) and may thus contribute to the difference in apoptotic responses observed in TK6 and WTK1 cells. Cytochrome *c*, APAF-1, and caspase 9 interact to form the apoptosome, leading to the proteolytic activation of caspase-9 and subsequent activation of the executioner caspase cascade. Consistently, the present data revealed that pro-caspase 9 protein levels were reduced in TK6 cells but not in WTK1 cells after NO• treatment, possibly due to failure of p53-dependent up-regulation of APAF-1 (24).

Bcl-2 family proteins are essential regulators of apoptosis in various *in vivo* and *in vitro* experimental models (50, 51). Our data show that NO• treatment resulted in reduction of Bcl-2 and Bcl-x/L proteins in TK6 but not in WTK1 cells, supporting the notion that mitochondrial function in apoptosis in these cells may be modulated by p53 through regulation of Bcl-2 family genes, which in turn control mitochondrial transition pores and release of mitochondrial proapoptotic factors. We consistently observed a higher release of mitochondrial cytochrome *c* (24), AIF, and endonuclease G (Fig. 4) in TK6 cells than in WTK1 cells. Further work will be required to determine whether mitochondrial dysfunction and apoptosis induced by NO• involve translocation of Bax and Bak proteins from cytosol to mitochondria in these cells.

p53-independent events such as NOXA expression and cytochrome *c* and Smac release may be involved in apoptotic processes through a complex network of p53-dependent and -independent transcriptional regulation and protein interactions. Mitochondria and downstream cascades modulated by Bcl-2 and IAP families are possible intersections of p53-dependent and -independent apoptosis. Consistent with another report (34), in an earlier related study, we found that the apoptotic response was reduced and delayed in WTK-1 cells compared with TK6 cells treated with NO• (24). This may in part be due to the direct involvement of p53 as a transcription factor as well as a "damage sensor" in the regulation of cell proliferation and death. In addition, the mutant p53 of WTK-1 cells may also exhibit so-called "gain of function" effects in apoptosis (52).

Taking into account presently accepted models of apoptosis, the present findings, along with our previous work (24), suggest that several signaling pathways leading to apoptosis are activated by NO• in TK6 cells, as summarized in Fig. 6. NO•-induced DNA damage is followed by activation of p53, which in turn up-regulates mitochondrial permeability proteins such as PUMA and NOXA and down-

regulates expression of Bcl-2 and Bcl-x/L proteins, leading to mitochondrial depolarization and release of the mitochondrial proapoptotic proteins cytochrome *c*, Smac, AIF, and endonuclease G. The impact of p53 activation is enhanced by concurrent down-regulation of MDM2. Cytochrome *c* binds to p53-regulated APAF-1, leading to recruitment and activation of initiator pro-caspase 9 to form the apoptosome, ultimately leading to activation of effector caspase 3, PARP cleavage, and apoptosis. Activated p53 also directly up-regulates expression of Fas/CD95, but not DR4 or -5, which subsequently activates caspases 8 and 10, followed by Bid cleavage and translocation onto mitochondria, further enhancing mitochondrial dysfunction. AIF and endonuclease G translocate from mitochondria into nuclei, resulting in caspase-independent apoptosis. p53 may further promote apoptosis through indirect down-regulation of the IAP proteins, which inhibit distinct caspases via HTRA2 and together with Smac eliminate IAP inhibition. Additionally, NO• may also damage mitochondria directly, although it is not possible to assess the effect of mitochondrial damage to the apoptotic phenotype in our current study. Despite the DNA damage, transcriptional activation of early genes, and release of apoptogenic factors caused by NO• treatment of WTK1 cells harboring mutant p53, no significant caspase 3 activation and PARP cleavage occurred in these cells. Thus, absence of functional p53 in WTK-1 cells is the most salient feature associated with the apoptotic response in this model.

ACKNOWLEDGMENTS

We thank Dr. Xin W. Wang for critical review of this manuscript and Esther Asaki for uploading original microarray data into GEO. Statistical analyses of microarray experiments were performed using BRB ArrayTools developed by Dr. Richard Simon and Amy Peng.[5]

REFERENCES

1. Kim PG, Zamora R, Petrosko P, Billiar TR. The regulatory role of nitric oxide in apoptosis. Int Immunopharmacol 2001;1:1421–41.
2. Hussain SP, Hofseth LJ, Harris CC. Radical causes of cancer. Nat Rev Cancer 2003;3:276–85.
3. Joza N, Kroemer G, Penninger JM. Genetic analysis of the mammalian cell death machinery. Trends Genet 2002;18:142–9.
4. Muller M, Wilder S, Bannasch D, et al. p53 activates the CD95 (APO-1/Fas) gene in response to DNA damage by anticancer drugs. J Exp Med 1998;188:2033–45.
5. Vogelstein B, Lane D, Levine AJ. Surfing the p53 network. Nature (Lond) 2000; 409:307–10.
6. Stewart ZA, Pietenpol JA. p53 signaling and cell cycle checkpoints. Chem Res Toxicol 2001;14:243–63.
7. Robles AI, Linke SP, Harris CC. The p53 network in lung carcinogenesis. Oncogene 2002;21:6898–907.
8. Polyak K, Xia Y, Zweier JL, Kinzler KW, Vogelstein B. A model for p53-induced apoptosis. Nature (Lond) 1997;389:300–5.
9. Miyashita T, Reed JC. Tumor suppressor p53 is a direct transcriptional activator of the human bax gene. Cell 1995;80:293–9.
10. Wu GS, Burns TF, McDonald ER 3rd, et al. KILLER/DR5 is a DNA damage-inducible p53-regulated death receptor gene. Nat Genet 1997;17:141–3.
11. Knudson CM, Tung KS, Tourtellotte WG, Brown GA, Korsmeyer SJ. Bax-deficient mice with lymphoid hyperplasia and male germ cell death. Science 1995;270:96–9.
12. Sheikh MS, Burns TF, Huang Y, et al. p53-dependent and -independent regulation of the death receptor KILLER/DR5 gene expression in response to genotoxic stress and tumor necrosis factor alpha. Cancer Res 1998;58:1593–8.
13. Owen-Schaub LB, Zhang W, Cusack JC, et al. Wild-type human p53 and a temperature-sensitive mutant induce Fas/APO-1 expression. Mol Cell Biol 1995;15:3032–40.
14. Fuchs EJ, McKenna KA, Bedi A. p53-dependent DNA damage-induced apoptosis requires Fas/APO-1-independent activation of CPP32β. Cancer Res 1997;57:2550–4.
15. Guan B, Yue P, Clayman GL, Sun SY. Evidence that the death receptor DR4 is a DNA damage-inducible, p53-regulated gene. J Cell Physiol 2001;188:98–105.
16. Nakano K, Vousden KH. PUMA, a novel proapoptotic gene, is induced by p53. Mol Cell 2001;7:683–94.
17. Yu J, Zhang L, Hwang PM, Kinzler KW, Vogelstein B. PUMA induces the rapid apoptosis of colorectal cancer cells. Mol Cell 2001;7:673–82.
18. Oda E, Ohki R, Murasawa H, et al. Noxa, a BH3-only member of the Bcl-2 family and candidate mediator of p53-induced apoptosis. Science (Wash DC) 2000;288:1053–8.
19. Moroni MC, Hickman ES, Denchi EL, et al. Apaf-1 is a transcriptional target for E2F and p53. Nat Cell Biol 2001;3:552–8.
20. Robles AI, Bemmels NA, Foraker AB, Harris CC. Apaf-1 is a transcriptional target of p53 in DNA damage-induced apoptosis. Cancer Res 2001;61:6660–4.
21. Jin S, Kalkum M, Overholtzer M, Stoffel A, Chait BT, Levine AJ. CIAP1 and the serine protease HTRA2 are involved in a novel p53-dependent apoptosis pathway in mammals. Genes Dev 2003;17:359–67.
22. Scorrano L, Korsmeyer SJ. Mechanisms of cytochrome c release by proapoptotic BCL-2 family members. Biochem Biophys Res Commun 2003;304:437–44.
23. Moll UM, Zaika A. Nuclear and mitochondrial apoptotic pathways of p53. FEBS Lett 2001;493:65–9.
24. Li CQ, Trudel LJ, Wogan GN. Nitric oxide-induced genotoxicity, mitochondrial damage, and apoptosis in human lymphoblastoid cells expressing wild-type and mutant p53. Proc Natl Acad Sci USA 2002;99:10364–9.
25. Du C, Fang M, Li Y, Li L, Wang X. Smac, a mitochondrial protein that promotes cytochrome c-dependent caspase activation by eliminating IAP inhibition. Cell 2000; 102:33–42.
26. Susin SA, Lorenzo HK, Zamzami N, et al. Molecular characterization of mitochondrial apoptosis-inducing factor. Nature (Lond) 1999;397:441–6.
27. Li LY, Luo X, Wang X. Endonuclease G is an apoptotic DNase when released from mitochondria. Nature (Lond) 2001;412:95–9.
28. Wang X, Yang C, Chai J, Shi Y, Xue D. Mechanisms of AIF-mediated apoptotic DNA degradation in Caenorhabditis elegans. Science (Wash DC) 2002;298:1587–92.
29. Holcik M, Gibson H, Korneluk RG. XIAP: apoptotic brake and promising therapeutic target. Apoptosis 2001;6:253–61.
30. Yang Y, Fang S, Jensen JP, Weissman AM, Ashwell JD. Ubiquitin protein ligase activity of IAPs and their degradation in proteasomes in response to apoptotic stimuli. Science (Wash DC) 2000;288:874–7.
31. Hoffman WH, Biade S, Zilfou JT, Chen J, Murphy M. Transcriptional repression of the anti-apoptotic survivin gene by wild type p53. J Biol Chem 2002;277:3247–57.
32. Mirza A, McGuirk M, Hockenberry TN, et al. Human survivin is negatively regulated by wild-type p53 and participates in p53-dependent apoptotic pathway. Oncogene 2002;21:2613–22.
33. Li CQ, Trudel LJ, Wogan GN. Genotoxicity, mitochondrial damage, and apoptosis in human lymphoblastoid cells exposed to peroxynitrite generated from SIN-1. Chem Res Toxicol 2002;15:527–35.
34. Yu Y, Little JB. p53 is involved in but not required for ionizing radiation-induced caspase-3 activation and apoptosis in human lymphoblast cell lines. Cancer Res 1998;58:4277–81.
35. Green LC, Wagner DA, Glogowski J, Skipper PL, Wishnok JS, Tannenbaum SR. Analysis of nitrate, nitrite, and [^{15}N]nitrate in biological fluids. Anal Biochem 1982;126:131–8.
36. Eisen MB, Spellman PT, Brown PO, Botstein D. Cluster analysis and display of genome-wide expression patterns. Proc Natl Acad Sci USA 1998;95:14863–8.
37. Hofseth LJ, Saito S, Hussain SP, et al. Nitric oxide-induced cellular stress and p53 activation in chronic inflammation. Proc Natl Acad Sci USA 2003;100:143–8.
38. Oren M. Decision making by p53: life, death and cancer. Cell Death Differ 2003; 10:431–42.
39. Wang X, Michael D, de Murcia G, Oren M. p53 activation by nitric oxide involves down-regulation of Mdm2. J Biol Chem 2002;277:15697–702.
40. Yu J, Wang Z, Kinzler KW, Vogelstein B, Zhang L. PUMA mediates the apoptotic response to p53 in colorectal cancer cells. Proc Natl Acad Sci USA 2003;100:1931–6.
41. Takekawa M, Adachi M, Nakahata A, et al. p53-inducible wip1 phosphatase mediates a negative feedback regulation of p38 MAPK-p53 signaling in response to UV radiation. EMBO J 2000;19:6517–26.
42. Flatt PM, Polyak K, Tang LJ, et al. p53-dependent expression of PIG3 during proliferation, genotoxic stress, and reversible growth arrest. Cancer Lett 2000;156:63–72.
43. Liebler DC, Aust AE, Wilson GL, Copeland ES. Reactive oxidants from nitric oxide, oxidants and cellular signalling, and repair of oxidative DNA damage: a Chemical Pathology Study Section workshop. Mol Carcinog 1998;22:209–20.
44. Korsmeyer SJ, Wei MC, Saito M, Weiler S, Oh KJ, Schlesinger PH. Pro-apoptotic cascade activates BID, which oligomerizes BAK or BAX into pores that result in the release of cytochrome c. Cell Death Differ 2000;7:1166–73.
45. Manderscheid M, Messmer UK, Franzen R, Pfeilschifter J. Regulation of inhibitor of apoptosis expression by nitric oxide and cytokines: relation to apoptosis induction in rat mesangial cells and raw 264.7 macrophages. J Am Soc Nephrol 2001;12:1151–63.
46. Kappler M, Kohler T, Kampf C, et al. Increased survivin transcript levels: an independent negative predictor of survival in soft tissue sarcoma patients. Int J Cancer 2001;95:360–3.
47. Sasaki H, Sheng Y, Kotsuji F, Tsang BK. Down-regulation of X-linked inhibitor of apoptosis protein induces apoptosis in chemoresistant human ovarian cancer cells. Cancer Res 2000;60:5659–66.
48. Yang QH, Church-Hajduk R, Ren J, Newton ML, Du C. Omi/HtrA2 catalytic cleavage of inhibitor of apoptosis (IAP) irreversibly inactivates IAPs and facilitates caspase activity in apoptosis. Genes Dev 2003;17:1487–96.
49. Daugas E, Susin SA, Zamzami N, et al. Mitochondrio-nuclear translocation of AIF in apoptosis and necrosis. FASEB J 2000;14:729–39.
50. Wei MC, Zong WX, Cheng EH, et al. Proapoptotic BAX and BAK: a requisite gateway to mitochondrial dysfunction and death. Science (Wash DC) 2001;292:727–30.
51. Sun XM, Bratton SB, Butterworth M, MacFarlane M, Cohen GM. Bcl-2 and Bcl-xL inhibit CD95-mediated apoptosis by preventing mitochondrial release of Smac/DIABLO and subsequent inactivation of X-linked inhibitor-of-apoptosis protein. J Biol Chem 2002;277:11345–51.
52. Sigal A, Rotter V. Oncogenic mutations of the p53 tumor suppressor: the demons of the guardian of the genome. Cancer Res 2000;60:6788–93.

[5] http://linus.nci.nih.gov/BRB-ArrayTools.html.